INTERNATIONAL JOURNAL OF
NUMERICAL ANALYSIS AND MODELING
Volume 14, Number 6, Pages 869–878

A QUADRILATERAL 'MINI' FINITE ELEMENT FOR THE STOKES PROBLEM USING A SINGLE BUBBLE FUNCTION

BISHNU P. LAMICHHANE

Abstract. We consider a quadrilateral 'mini' finite element for approximating the solution of Stokes equations using a quadrilateral mesh. We use the standard bilinear finite element space enriched with element-wise defined bubble functions for the velocity and the standard bilinear finite element space for the pressure space. With a simple modification of the standard bubble function we show that a single bubble function is sufficient to ensure the inf-sup condition. We have thus improved an earlier result on the quadrilateral 'mini' element, where more than one bubble function are used to get the stability.

Key words. Stokes equations, mixed finite elements, Mini finite element, inf-sup condition, bubble function.

1. Introduction

A very simple finite element method for the Stokes problem for a simplicial mesh is presented by Arnold, Brezzi and Frotin [1], where the velocity space is discretised by using the standard linear finite element space enriched with element-wise bubble functions and the pressure space is discretised by using the standard linear finite element space. The enrichment of the velocity space is done to ensure the stability of the finite element method, and this increases one vector degree of freedom per element. An extension of the finite element method to the quadrilateral mesh is done by Bai [2], where the author enriches the velocity space with more than a single vector bubble function per element. The inf-sup condition is proved by using a macro element technique [9], where a single quadrilateral element is used as a macro element.

In this article we show that with a small modification of the standard bubble function we can get the stability just by using a single vector bubble function per element. The main difference with the technique proposed by Bai [2] is that it is not possible to show the inf-sup condition using a single quadrilateral element as a macro element. We need to use a macro element consisting of four quadrilateral elements to prove the inf-sup condition in our situation. Another relevant finite element method is presented by Lamichhane [8], where two different meshes are used to discretise the velocity and the pressure space, and a single vector bubble degree of freedom per element is used to get the stability. The pressure space is discretised by the space of piecewise constant functions on the dual mesh. However, the main difficulty of the technique presented by Lamichhane [8] is that the bubble function is obtained by multiplying the standard bubble function by the gradient of a bilinear basis function, and hence the bubble function cannot be defined on a reference element. The standard bubble function on the unit square is the lowest degree polynomial which vanishes on the boundary of the square. Here we modify the standard bubble function [1, 2] to get stability of the numerical scheme by using

Received by the editors July 16, 2015 and, in revised form, July 17, 2017.
2000 *Mathematics Subject Classification.* 65N30, 65N15, 74B10.

a single vector bubble function per element with a continuous pressure approximation. We also investigate two choices of bubble functions, where both of them can be defined on a reference element. Thus the main contribution of the paper is to introduce a modification of the standard bubble function so that the discrete velocity space can be enriched by a single bubble function per element to satisfy the inf-sup condition for a quadrilateral mesh. The idea can easily be extended to the three-dimensional case.

2. Stokes equations

This section is devoted to the introduction of the boundary value problem of the Stokes equations. Let Ω in $\mathbb{R}^2$, be a bounded domain with polygonal boundary Γ. For a prescribed body force $\boldsymbol{f} \in [L^2(\Omega)]^2$, the Stokes equations with homogeneous Dirichlet boundary condition in Γ reads

$$\begin{array}{lcll} -\nu\Delta\boldsymbol{u} + \nabla p & = & \boldsymbol{f} & \text{in} \quad \Omega \\ \operatorname{div}\boldsymbol{u} & = & 0 & \text{in} \quad \Omega \end{array} \tag{1}$$

with $\boldsymbol{u} = \boldsymbol{0}$ on Γ, where $\boldsymbol{u}$ is the velocity, p is the pressure, and ν denotes the viscosity of the fluid.

Here we use standard notations $L^2(\Omega)$, $H^1(\Omega)$ and $H^1_0(\Omega)$ for Sobolev spaces, see [4, 6] for details. Let $\boldsymbol{V} := [H^1_0(\Omega)]^2$ be the vector Sobolev space with inner product $(\cdot,\cdot)_{1,\Omega}$ and norm $\|\cdot\|_{1,\Omega}$ defined in the standard way: $(\boldsymbol{u},\boldsymbol{v})_{1,\Omega} := \sum_{i=1}^2 (u_i, v_i)_{1,\Omega}$, and the norm being induced by this inner product. We also define another subspace M of $L^2(\Omega)$ as

$$P = \left\{ q \in L^2(\Omega) : \int_\Omega q\, dx = 0 \right\}.$$

The weak formulation of the Stokes equations is to find $(\boldsymbol{u}, p) \in \boldsymbol{V} \times P$ such that

$$\begin{array}{llll} \nu \int_\Omega \nabla\boldsymbol{u} : \nabla\boldsymbol{v}\, dx & + \int_\Omega \operatorname{div} v\, p\, dx & = \ell(\boldsymbol{v}), & \boldsymbol{v} \in \boldsymbol{V}, \\ \int_\Omega \operatorname{div}\boldsymbol{u}\, q\, dx & & = 0, & q \in P, \end{array} \tag{2}$$

where $\ell(\boldsymbol{v}) = \int_\Omega \boldsymbol{f} \cdot \boldsymbol{v}\, dx$. It is well-known that the weak formulation of the Stokes problem is well-posed [7]. In fact, if the domain Ω is convex, and $\boldsymbol{f} \in [L^2(\Omega)]^2$, we have $\boldsymbol{u} \in [H^2(\Omega)]^2$, $p \in H^1(\Omega)$ and the a priori estimate holds

$$\|\boldsymbol{u}\|_{2,\Omega} + \|p\|_{1,\Omega} \le C\|\boldsymbol{f}\|_{0,\Omega},$$

where the constant C depends on the domain Ω.

3. Finite element discretizations

We consider a quasi-uniform triangulation $\mathcal{T}_h$ of the polygonal domain Ω, where $\mathcal{T}_h$ consists of parallelograms. The finite element meshes are defined by maps from the reference square $\hat{K} = (0,1)^2$ to the actual parallelogram $K \in \mathcal{T}_h$. Let $\mathcal{Q}_1(\hat{K})$ be the space of bilinear polynomials in $\hat{K}$. We start with the finite element space of continuous functions whose restrictions to an element K are obtained by maps of *bilinear* functions from the reference element:

$$S_h := \left\{ v_h \in H^1_0(\Omega),\ v_h|_K = \hat{v}_h \circ F_K^{-1}, \hat{v}_h \in \mathcal{Q}_1(\hat{K}),\ K \in \mathcal{T}_h \right\}, \tag{3}$$

where $F_K : \hat{K} \to K$ is an affine mapping.

Remark 1. *For a convex quadrilateral the mapping $F_K : \hat{K} \to K$ is an isoparametric map, which may not be an affine mapping. The mapping becomes an affine mapping if K is a parallelogram.*

Let b_K be a bi-variate polynomial of $\boldsymbol{x} \in \mathbb{R}^2$ with $b_K = 0$ on ∂K, $b_K(\boldsymbol{x}_K) = 1$ and positive on K, where $\boldsymbol{x}_K \in \mathbb{R}^2$ is the centroid of K. This is called a bubble function corresponding to the element $K \in \mathcal{T}_h$. Defining the space of bubble functions

$$B_h := \{b_h \in C^0(\Omega) : b_h|_K = c_K b_K,\ c_K \in \mathbb{R},\ K \in \mathcal{T}_h\}, \tag{4}$$

we introduce our finite element space for velocity as $\boldsymbol{V}_h = [S_h \oplus B_h]^2$. The finite element space for the pressure is taken as the standard bilinear finite element space

$$S_h^* := \left\{ v_h \in L_0^2(\Omega) \cap H^1(\Omega),\ v_h|_K = \hat{v}_h \circ F_K^{-1}, \hat{v}_h \in \mathcal{Q}_1(\hat{K}),\ K \in \mathcal{T}_h \right\} . \tag{5}$$

Then, the finite element approximation of (2) is defined as a solution to the following problem: find $(\boldsymbol{u}_h, p_h) \in \boldsymbol{V}_h \times S_h^*$ such that

$$\begin{array}{lclll} a(\boldsymbol{u}_h, \boldsymbol{v}_h) + b(\boldsymbol{v}_h, p_h) & = & \ell(\boldsymbol{v}_h), & \boldsymbol{v}_h & \in \boldsymbol{V}_h, \\ b(\boldsymbol{u}_h, q_h) & = & 0, & q_h & \in S_h^*. \end{array} \tag{6}$$

We need the following conditions to prove that there is a unique solution of the discrete problem (6) and the discrete solution converges optimally to the continuous solution.

(1) The bilinear forms $a(\cdot,\cdot)$ on $\boldsymbol{V}_h \times \boldsymbol{V}_h$ and $b(\cdot,\cdot)$ on $\boldsymbol{V}_h \times S_h^*$ are continuous.
(2) The bilinear form $a(\cdot,\cdot)$ on $\boldsymbol{V}_h \times \boldsymbol{V}_h$ is elliptic.
(3) There exists a constant $\beta > 0$ independent of the mesh-size such that for any $q_h \in S_h^*$, we have

$$\sup_{\boldsymbol{v}_h \in \boldsymbol{V}_h} \frac{b(\boldsymbol{v}_h, q_h)}{\|\boldsymbol{v}_h\|_{1,\Omega}} \geq \beta \|q_h\|_{0,\Omega}. \tag{7}$$

The constant β with the property

$$\beta = \inf_{q_h \in S_h^*} \sup_{\boldsymbol{v}_h \in \boldsymbol{V}_h} \frac{b(\boldsymbol{v}_h, q_h)}{\|\boldsymbol{v}_h\|_{1,\Omega}, \|q_h\|_{0,\Omega}} \tag{8}$$

is called the inf-sup constant.

4. The Macro-Element Technique

We prove the inf-sup condition (7) using a macro-element technique proposed by Stenberg [9]. A macro-element M is a connected set of elements in $\mathcal{T}_h$. Moreover, two macro-elements M_1 and M_2 are said to be equivalent if they can be mapped continuously onto each other [9]. We define the following three spaces associated with the macro-element M_i:

$$\begin{aligned} \boldsymbol{V}_h^i &= [H_0^1(M_i)]^2 \cap \boldsymbol{V}, \\ S_h^i &= \left\{ v_h \in H^1(M_i),\ v_h|_K = \hat{v}_h \circ F_K^{-1}, \hat{v}_h \in \mathcal{Q}_1(\hat{K}),\ K \in \mathcal{T}_h,\ K \subset M_i \right\}, \text{ and} \\ B_i &= \left\{ q_h \in S_h^i \,|\, b(\boldsymbol{v}_h, q_h) = 0,\ \boldsymbol{v}_h \in \boldsymbol{V}_h^i \right\}. \end{aligned}$$

Moreover, we denote by Γ_h the set of all edges in $\mathcal{T}_h$ interior to Ω. The macro-element partition $\mathcal{M}_h$ of Ω then consists of macro-elements $\{M_i\}_{i=1}^N$ with $\bar{\Omega} = \bigcup_{i=1}^N \bar{M}_i$. The macro-element technique is given by the following theorem [9].

Theorem 2. *Suppose that there is a fixed set of equivalence classes $\mathcal{E}_j$, $j = 1, \cdots, q$, of macro-elements, a positive integer L, and a macro-element partition $\mathcal{M}_h$ such that*

(M1) *For each $M_i \in \mathcal{E}_j$, $j = 1, \cdots, q$, the space B_i is one-dimensional, consisting of functions that are constant on M_i.*
(M2) *Each $M_i \in \mathcal{M}_h$ belongs to one of the classes $\mathcal{E}_j$, $j = 1, \cdots, q$.*

(M3) *Each $T \in \mathcal{T}_h$ is contained in at least one and not more than L macro-elements of $\mathcal{M}_h$.*
(M4) *Each $e \in \Gamma_h$ is contained in the interior of at least one and not more than L macro-elments of $\mathcal{M}_h$.*

Then the inf-sup condition (7) *is satisfied.*

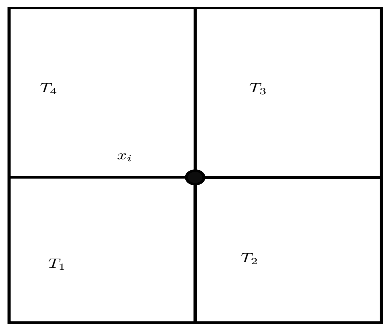

FIGURE 1. The set M_i, where four elements of $\mathcal{T}_h$ touch the vertex $\boldsymbol{x}_i$.

In the following we consider a macro-element consisting of four squares as shown in Figure 1. With this partition of macro-elements we can see that Assumptions (M2)–(M4) are all satisfied. We now show that the proof of Assumption (M1) depends on the choice of bubble functions. We note that the earlier approach by Bai [2] also uses the macro-element technique but use a single quadrilateral element as a macro element. In contrast to that earlier approach we need to use a macro-element consisting of four quadrilateral elements.

4.1. Choice of bubble functions. For simplicity of calculation we assume that M_i is a parallelogram so that there is an invertible affine mapping $F_i : \hat{S} \to M_i$, which transforms the square $\hat{S} = [-1, 1]^2$ to M_i with the property

$$\begin{bmatrix} x \\ y \end{bmatrix} = A_i \begin{bmatrix} \xi \\ \eta \end{bmatrix} + \begin{bmatrix} x_0 \\ y_0 \end{bmatrix}, \tag{9}$$

where A_i is a 2 by 2 matrix, $(x, y) \in M_i$ and $(\xi, \eta) \in \hat{S}$. Let $V_h^i = \operatorname{span}\{\phi_k\}_{k=1}^5$, $\boldsymbol{V}_h^i = [V_h^i]^2$ and $S_h^i = \operatorname{span}\{\varphi_k\}_{k=1}^9$. We use the notation $\hat{\phi}_k$ and $\hat{\varphi}_k$ to denote corresponding basis functions on the square $\hat{S}$, where $\hat{\phi}_k$ and $\hat{\varphi}_k$ are functions of ξ and η. We have shown the numbering of functions $\hat{\phi}_k$ and $\hat{\varphi}_j$ on the reference square $\hat{S}$ in Figure 2, where we have used big circles for the functions in $\boldsymbol{V}_h$, and small circles for functions in S_h^*.

Let $\boldsymbol{v}_h \in \boldsymbol{V}_h^i$ with $\boldsymbol{v}_h = \sum_{k=1}^5 \boldsymbol{v}_k \phi_k$ and $\boldsymbol{v}_k \in \mathbb{R}^2$. Then

$$b(\boldsymbol{v}_h, q_h) = \int_{M_i} \nabla \cdot \boldsymbol{v}_h \, q_h \, dx = \sum_{k=1}^{5} \int_{M_i} \boldsymbol{v}_k \cdot \nabla \phi_k \, q_h \, dx.$$

Using a chain rule we write

$$\nabla \phi_k = A_i^{-T} \left(\hat{\nabla} \hat{\phi}_k \circ F_i^{-1} \right),$$

where $\hat{\nabla}$ denotes the gradient on the reference square $\hat{S}$. Let $q_h = \sum_{j=1}^{9} q_j \varphi_j$, and thus

$$\int_{M_i} \nabla \cdot \boldsymbol{v}_h \, q_h \, dx = \sum_{k=1}^{5} \sum_{j=1}^{9} q_j \boldsymbol{v}_k \cdot \int_{M_i} \nabla \phi_k \, q_j \varphi_j \, dx$$
$$= |\det A_i| \sum_{k=1}^{5} \sum_{j=1}^{9} q_j \boldsymbol{v}_k \cdot \int_{\hat{S}} A_i^{-T} \hat{\nabla} \hat{\phi}_k \hat{\varphi}_j \, d\hat{x}.$$

We see that we can find a matrix $\tilde{D}$ such that

$$\int_{M_i} \nabla \cdot \boldsymbol{v}_h \, q_h \, dx = \vec{q}^T \tilde{D} \vec{v},$$

where

$$\vec{q} = \begin{bmatrix} q_1 \\ q_2 \\ \vdots \\ q_9 \end{bmatrix}, \quad \text{and} \quad \vec{v} = \begin{bmatrix} \boldsymbol{v}_1 \\ \boldsymbol{v}_2 \\ \vdots \\ \boldsymbol{v}_5 \end{bmatrix} = \begin{bmatrix} v_1 \\ v_2 \\ v_3 \\ v_4 \\ \vdots \\ v_9 \\ v_{10} \end{bmatrix}.$$

Thus we need to show that the rank of the matrix $\tilde{D}$ is 8 in order to prove that the dimension of the space B_i is one.

Since A_i is an invertible matrix, the rank of the matrix will be unchanged if we replace M_i by the reference element $\hat{S}$, so that we want to investigate the rank of the matrix $D \in \mathbb{R}^{9\times 10}$, where the jth row of D is

$$\Big[\int_{\hat{S}} \partial_\xi \hat{\phi}_1 \hat{\varphi}_j \, d\hat{x}, \int_{\hat{S}} \partial_\eta \hat{\phi}_1 \hat{\varphi}_j \, d\hat{x}, \int_{\hat{S}} \partial_\xi \hat{\phi}_2 \hat{\varphi}_j \, d\hat{x}, \int_{\hat{S}} \partial_\eta \hat{\phi}_2 \hat{\varphi}_j \, d\hat{x}, \cdots,$$
$$\int_{\hat{S}} \partial_\xi \hat{\phi}_5 \hat{\varphi}_j \, d\hat{x}, \int_{\hat{S}} \partial_\eta \hat{\phi}_5 \hat{\varphi}_j \, d\hat{x}\Big].$$

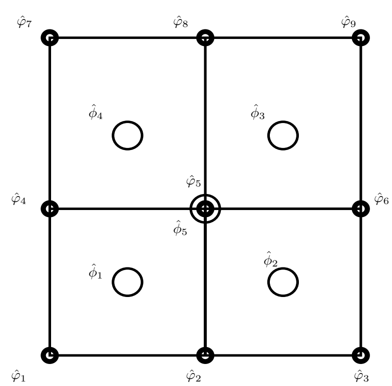

FIGURE 2. The numbering of functions $\hat{\phi}_k$ and $\hat{\varphi}_j$ on the reference square $\hat{S}$.

4.1.1. Standard bubble functions. Consider the unit square $K = (-1,1)^2$ in two dimensions. We start with the standard choice of the bubble function $b_K = (1-x^2)(1-y^2)$. The matrix D is explicitly computed as

$$D = \begin{bmatrix} \frac{2}{9} & \frac{2}{9} & 0 & 0 & 0 & 0 & 0 & 0 & \frac{1}{12} & \frac{1}{12} \\ -\frac{2}{9} & \frac{2}{9} & \frac{2}{9} & \frac{2}{9} & 0 & 0 & 0 & 0 & 0 & \frac{1}{3} \\ 0 & 0 & -\frac{2}{9} & \frac{2}{9} & 0 & 0 & 0 & 0 & -\frac{1}{12} & \frac{1}{12} \\ \frac{2}{9} & -\frac{2}{9} & 0 & 0 & 0 & 0 & \frac{2}{9} & \frac{2}{9} & \frac{1}{3} & 0 \\ -\frac{2}{9} & -\frac{2}{9} & \frac{2}{9} & -\frac{2}{9} & \frac{2}{9} & \frac{2}{9} & -\frac{2}{9} & \frac{2}{9} & 0 & 0 \\ 0 & 0 & -\frac{2}{9} & -\frac{2}{9} & -\frac{2}{9} & \frac{2}{9} & 0 & 0 & -\frac{1}{3} & 0 \\ 0 & 0 & 0 & 0 & 0 & 0 & \frac{2}{9} & -\frac{2}{9} & \frac{1}{12} & -\frac{1}{12} \\ 0 & 0 & 0 & 0 & \frac{2}{9} & -\frac{2}{9} & -\frac{2}{9} & -\frac{2}{9} & 0 & -\frac{1}{3} \\ 0 & 0 & 0 & 0 & -\frac{2}{9} & -\frac{2}{9} & 0 & 0 & -\frac{1}{12} & -\frac{1}{12} \end{bmatrix}.$$

We compute the rank of this matrix using MAPLE and obtain it to be 7. Thus in this case the dimension of the space B_i will be two. Hence there is no hope of getting the inf-sup condition for this choice of the bubble function.

4.1.2. The first choice of bubble functions. In the next step, we again take $K = (-1,1)^2$ and consider the bubble function

$$b_K = 4\varphi_K(1-x^2)(1-y^2),$$

where φ_K is the standard bilinear basis function corresponding to the lower-left corner of the square K. Since $\varphi_K = \frac{1}{4}(1-x)(1-y)$, the bubble function b_K on the reference square K can be defined as

$$b_K = (1-x)(1-y)(1-x^2)(1-y^2).$$

Defined in this way the bubble function b_K does not depend on the local numbering of the vertices of K. In this case, the matrix D has rank 8, and is computed as

$$D = \begin{bmatrix} \frac{4}{15} & \frac{4}{15} & 0 & 0 & 0 & 0 & 0 & 0 & \frac{1}{12} & \frac{1}{12} \\ -\frac{4}{15} & \frac{8}{45} & \frac{4}{15} & \frac{4}{15} & 0 & 0 & 0 & 0 & 0 & \frac{1}{3} \\ 0 & 0 & -\frac{4}{15} & \frac{8}{45} & 0 & 0 & 0 & 0 & -\frac{1}{12} & \frac{1}{12} \\ \frac{8}{45} & -\frac{4}{15} & 0 & 0 & 0 & 0 & \frac{4}{15} & \frac{4}{15} & \frac{1}{3} & 0 \\ -\frac{8}{45} & -\frac{8}{45} & \frac{8}{45} & -\frac{4}{15} & \frac{4}{15} & \frac{4}{15} & -\frac{4}{15} & \frac{8}{45} & 0 & 0 \\ 0 & 0 & -\frac{8}{45} & -\frac{8}{45} & -\frac{4}{15} & \frac{8}{45} & 0 & 0 & -\frac{1}{3} & 0 \\ 0 & 0 & 0 & 0 & 0 & 0 & \frac{8}{45} & -\frac{4}{15} & \frac{1}{12} & -\frac{1}{12} \\ 0 & 0 & 0 & 0 & \frac{8}{45} & -\frac{4}{15} & -\frac{8}{45} & -\frac{8}{45} & 0 & -\frac{1}{3} \\ 0 & 0 & 0 & 0 & -\frac{8}{45} & -\frac{8}{45} & 0 & 0 & -\frac{1}{12} & -\frac{1}{12} \end{bmatrix}.$$

Remark 3. *We have used the gradient of the bilinear function φ_K to construct a vector bubble function associated with the element K in* [8]. *Since the construction of the bubble function using the gradient of φ_K cannot be done on a reference element, this new bubble function is computationally much easier.*

4.1.3. The second choice of bubble functions. It is interesting to see if we can multiply the bubble function by a linear function and obtain the stability. For this purpose we can choose a bubble function on the unit square $(-1,1)^2$ as

$$b_K = (a + bx + cy)(1 - x^2)(1 - y^2), \quad abc \neq 0.$$

For simplicity we choose

$$b_K = \frac{1}{4}(4 + x + y)(1 - x^2)(1 - y^2).$$

We note that the factor $1/4$ is used to force the value of the bubble function at the centroid of the square to be 1. The resulting matrix D has also rank 8 in this case, and hence the dimension of the space B_i is one. Moreover, the matrix D is computed as

$$D = \begin{bmatrix}
\frac{19}{90} & \frac{19}{90} & 0 & 0 & 0 & 0 & 0 & 0 & \frac{1}{12} & \frac{1}{12} \\
-\frac{19}{90} & \frac{7}{30} & \frac{19}{90} & \frac{19}{90} & 0 & 0 & 0 & 0 & 0 & \frac{1}{3} \\
0 & 0 & -\frac{19}{90} & \frac{7}{30} & 0 & 0 & 0 & 0 & -\frac{1}{12} & \frac{1}{12} \\
\frac{7}{30} & -\frac{19}{90} & 0 & 0 & 0 & 0 & \frac{19}{90} & \frac{19}{90} & \frac{1}{3} & 0 \\
-\frac{7}{30} & -\frac{7}{30} & \frac{7}{30} & -\frac{19}{90} & \frac{19}{90} & \frac{19}{90} & -\frac{19}{90} & \frac{7}{30} & 0 & 0 \\
0 & 0 & -\frac{7}{30} & -\frac{7}{30} & -\frac{19}{90} & \frac{7}{30} & 0 & 0 & -\frac{1}{3} & 0 \\
0 & 0 & 0 & 0 & 0 & 0 & \frac{7}{30} & -\frac{19}{90} & \frac{1}{12} & -\frac{1}{12} \\
0 & 0 & 0 & 0 & \frac{7}{30} & -\frac{19}{90} & -\frac{7}{30} & -\frac{7}{30} & 0 & -\frac{1}{3} \\
0 & 0 & 0 & 0 & -\frac{7}{30} & -\frac{7}{30} & 0 & 0 & -\frac{1}{12} & -\frac{1}{12}
\end{bmatrix}.$$

Remark 4. *The proof of stability is presented for the two-dimensional case. However, this can be extended to the three-dimensional case without a major change.*

Remark 5. *It is interesting to see if we can use a quadratic function symmetric about the centroid of the element to multiply the standard bubble function. To check this we use a bubble function on the reference square $K = (-1,1)^2$ defined as*

$$b_K = \frac{1}{64}(x^2 + y^2 + 64)(1 - x^2)(1 - y^2),$$

and compute the matrix D. In this case, the rank of the matrix D is just 7, and hence the dimension of the space B_i is 2.

An immediate consequence of the above discussion is the well-posedness of the discrete problem (6) for the above two choices of bubble functions. From the theory of saddle point problem, see, e.g., [5], we have the following theorem.

Theorem 6. *The discrete problem* (6) *has exactly one solution $(\boldsymbol{u}_h, p_h) \in \boldsymbol{V}_h \times S_h^*$, which is uniformly stable with respect to the data $\boldsymbol{f}$, and there exists a constant C independent of the mesh-size h such that*

$$\|\boldsymbol{u}_h\|_{1,\Omega} + \|p_h\|_{0,\Omega} \leq C\|\boldsymbol{f}\|_{0,\Omega}.$$

The convergence theory is provided by an abstract result about the approximation of saddle point problems, see [5].

Theorem 7. *Assume that $(\boldsymbol{u}, p)$ and $(\boldsymbol{u}_h, p_h)$ be the solutions of problems* (2) *and* (6)*, respectively. Then, we have the following error estimate:*

$$\|\boldsymbol{u} - \boldsymbol{u}_h\|_{1,\Omega} + \|p - p_h\|_{0,\Omega} \leq C\left(\inf_{\boldsymbol{v}_h \in \boldsymbol{V}_h} \|\boldsymbol{u} - \boldsymbol{v}_h\|_{1,\Omega} + \inf_{q_h \in S_h^*} \|p - q_h\|_{0,\Omega}\right). \tag{10}$$

5. Numerical Results

In this section we present two numerical experiments to verify the optimal a priori error estimate and some numerical experiments to verify the inf-sup condition for the proposed finite element scheme. For both examples we consider a simple unit square $\Omega = (0,1)^2$. For both examples we consider a uniform initial triangulation consisting of four squares.

First example. For the first example we choose the exact solution $\boldsymbol{u} = (u_1, u_2)$ as

$$u_1 = -2\,x^2\,y\,(2\,y-1)\,(x-1)^2\,(y-1)\,, \quad u_2 = 2\,x\,y^2\,(2\,x-1)\,(x-1)\,(y-1)^2.$$

We use the kinematic viscosity $\nu = 1$. The exact solution for the pressure is chosen as

$$p = x(1-x)(1-2y),$$

so that $p \in L^2_0(\Omega)$. The exact solution $\boldsymbol{u}$ satisfies the homogeneous Dirichlet boundary condition on $\partial\Omega$, and the right hand side function $\boldsymbol{f}$ is computed by using the exact solution $\boldsymbol{u}$ and the pressure p. We have presented the errors in the velocity and the pressure approximation using the H^1-norm and the L^2- norm, respectively in Table 1 for the first choice of the bubble function, and in Table 2 for the second choice of the bubble function. We note that the standard choice of the bubble function leads to a singular matrix. From the presented tables we can see the optimal convergence of the velocity approximation in the H^1 and L^2-norms, and a super-convergence result for the pressure in the L^2-norm. As we expect a convergence rate of order 1 for the pressure approximation in the L^2-norm but get a better approximation of order 1.5, this is a super-convergence. This better convergence is due to the fact that we have used the standard continuous bilinear finite element space for the pressure approximation. We can also observe that all errors are smaller for the second choice of bubble functions.

Table 1. Discretization errors for the velocity and pressure, Example 1 (First choice).

level l	# elem.	$\|u-u_h\|_{1,\Omega}$		$\|u-u_h\|_{0,\Omega}$		$\|p-p_h\|_{0,\Omega}$	
1	16	3.23129e-02		3.03116e-03		1.76150e-02	
2	64	1.58286e-02	1.03	8.24246e-04	1.88	7.00356e-03	1.33
3	256	7.79938e-03	1.02	2.06421e-04	2.00	2.50753e-03	1.48
4	1024	3.87699e-03	1.01	5.12144e-05	2.01	8.78516e-04	1.51
5	4096	1.93346e-03	1.00	1.27289e-05	2.01	3.08875e-04	1.51
6	16384	9.65545e-04	1.00	3.17131e-06	2.00	1.08856e-04	1.50

Table 2. Discretization errors for the velocity and pressure, Example 1 (Second choice).

level l	# elem.	$\|u-u_h\|_{1,\Omega}$		$\|u-u_h\|_{0,\Omega}$		$\|p-p_h\|_{0,\Omega}$	
1	16	3.16876e-02		2.89325e-03		1.17765e-02	
2	64	1.56503e-02	1.02	7.90369e-04	1.87	4.31789e-03	1.45
3	256	7.75922e-03	1.01	1.99983e-04	1.98	1.44890e-03	1.58
4	1024	3.86716e-03	1.00	4.99365e-05	2.00	4.93948e-04	1.55
5	4096	1.93102e-03	1.00	1.24544e-05	2.00	1.71287e-04	1.53
6	16384	9.64934e-04	1.00	3.10849e-06	2.00	5.99594e-05	1.51

Second example. For the second example we consider an exact solution given in [3], where the exact solution for the velocity $\boldsymbol{u} = (u_1, u_2)$ is given by

$$u_1 = x + x^2 - 2\,xy + x^3 - 3\,xy^2 + x^2y, \quad u_2 = -y - 2\,xy + y^2 - 3\,x^2y + y^3 - xy^2,$$

and the exact solution for the pressure is given by

$$p = xy + x + y + x^3y^2 - \frac{4}{3}.$$

We use the kinematic viscosity $\nu = 1$ and the exact solution to compute the right-hand side function $\boldsymbol{f}$. As in the first example we compute the errors in the velocity and the pressure approximation using the H^1–norm and the L^2- norm, respectively. The numerical results are tabulated in Tables 3 and 4 for the two choices of bubble functions, respectively. As in the first example, we can see the optimal convergence rates for the velocity approximation in H^1 and L^2-norms, and a better convergence rate for the pressure in L^2-norm. We also observe that all errors are smaller for the second choice of bubble functions although the difference is quite small in this example.

TABLE 3. Discretization errors for the velocity and pressure, Example 2 (First choice).

level l	# elem.	$\\|u-u_h\\|_{1,\Omega}$		$\\|u-u_h\\|_{0,\Omega}$		$\\|p-p_h\\|_{0,\Omega}$	
1	16	6.96126e-01		3.33821e-02		2.25132e+00	
2	64	3.39100e-01	1.04	8.37772e-03	1.99	5.58680e-01	2.01
3	256	1.66684e-01	1.02	2.09556e-03	2.00	1.59539e-01	1.81
4	1024	8.26546e-02	1.01	5.24458e-04	2.00	4.49273e-02	1.83
5	4096	4.11633e-02	1.01	1.31193e-04	2.00	1.28191e-02	1.81
6	16384	2.05425e-02	1.00	3.28081e-05	2.00	3.80370e-03	1.75

TABLE 4. Discretization errors for the velocity and pressure, Example 2 (Second choice).

level l	# elem.	$\\|u-u_h\\|_{1,\Omega}$		$\\|u-u_h\\|_{0,\Omega}$		$\\|p-p_h\\|_{0,\Omega}$	
1	16	6.96024e-01		3.23184e-02		5.93926e+00	
2	64	3.35337e-01	1.05	7.82819e-03	2.05	4.04732e-01	3.88
3	256	1.65795e-01	1.02	1.97572e-03	1.99	6.07983e-02	2.73
4	1024	8.24467e-02	1.01	4.97135e-04	1.99	1.78268e-02	1.77
5	4096	4.11137e-02	1.00	1.24714e-04	2.00	5.88206e-03	1.60
6	16384	2.05304e-02	1.00	3.12328e-05	2.00	1.98964e-03	1.56

6. Conclusion

In this contribution we present a finite element method for Stokes equations using continuous bilinear finite elements enriched with bubble functions for the velocity approximation and continuous bilinear finite elements for the pressure. In contrast to an earlier contribution we show that a single vector bubble function per element is enough to guarantee the stability of the discrete linear system. The numerical results also demonstrate the optimal convergence rates for the velocity and pressure approximation.

References

[1] D. Arnold, F. Brezzi, M. Fortin, A stable finite element for the Stokes equations, Calcolo 21 (1984) 337–344.

[2] W. Bai, A quadrilateral 'mini' finite element for the Stokes problem, Computer Methods in Applied Mechanics and Engineering 143 (1997) 41–47.

[3] P. Bochev, C. Dohrmann, M. Gunzburger, Stabilization of low-order mixed finite elements for the Stokes equations, SIAM Journal on Numerical Analysis 44 (2006) 82–101.

[4] S. Brenner, L. Scott, The Mathematical Theory of Finite Element Methods, Springer–Verlag, New York, 1994.

[5] F. Brezzi, M. Fortin, Mixed and hybrid finite element methods, Springer–Verlag, New York, 1991.

[6] P. Ciarlet, The Finite Element Method for Elliptic Problems, North Holland, Amsterdam, 1978.

[7] V. Girault, P.-A. Raviart, Finite Element Methods for Navier-Stokes Equations, Springer-Verlag, Berlin, 1986.

[8] B. Lamichhane, A mixed finite element method for nearly incompressible elasticity and Stokes equations using primal and dual meshes with quadrilateral and hexahedral grids, Journal of Computational and Applied Mathematics 260 (2014) 356–363.

[9] R. Stenberg, Error analysis of some finite element methods for the Stokes problem, Mathematics of Computation 54 (1990) 495–508.

School of Mathematical and Physical Sciences, University of Newcastle, Callaghan, NSW 2308
E-mail: Bishnu.Lamichhane@newcastle.edu.au